

The Keck Interferometer Nuller: System Architecture and Laboratory Performance

E. Serabyn, A. Booth, M. M. Colavita, M. Creech-Eakman, S. Crawford, J. Garcia, R. Johnson,
E. Hovland, C. Koresko, R. Ligon, S. R. Martin, B. Mennesson, J. Moore, D. Palmer, C. Paine,
M. Shao, M. Swain, R. Smythe, and G. Vasisht
Jet Propulsion Laboratory, California Institute of Technology, Pasadena, CA 91109, USA

ABSTRACT

The first high-dynamic-range interferometric mode planned to come on line at the Keck Observatory is mid-infrared nulling. This observational mode, which is based on the cancellation of the on-axis starlight arriving at the twin Keck telescopes, will be used to examine nearby stellar systems for the presence of circumstellar exozodiacal emission. This paper describes the system level layout of the Keck Interferometer Nuller (KIN), as well as the final performance levels demonstrated in the laboratory integration and test phase at the Jet Propulsion Laboratory prior to shipment of the nuller hardware to the Keck Observatory in mid-June 2004. On-sky testing and observation with the mid-infrared nuller are slated to begin in August 2004.

1. INTRODUCTION

The primary goal of the Keck Interferometer Nuller is the detection and characterization of exo-zodiacal dust disks around nearby main sequence stars. The characterization of such dust disks is a vital preliminary step on the road to the direct detection of terrestrial planets with eventual space missions such as NASA's Terrestrial Planet Finder¹ and ESA's Darwin² missions. This is especially true in the case of the thermal infrared, where exo-zodiacal emission is potentially much brighter than the emission from terrestrial planetary analogs.

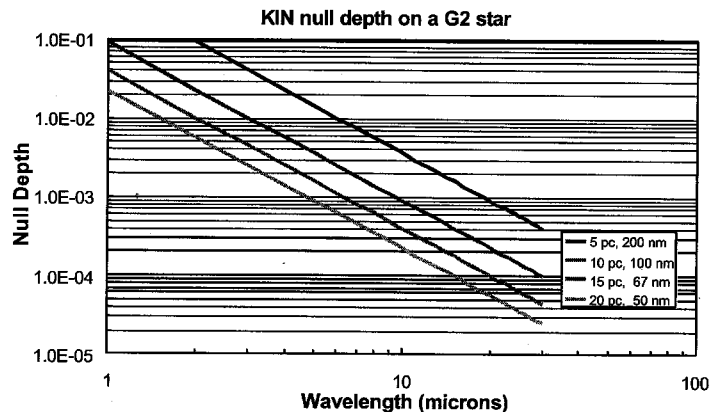


Figure 1. Null depths vs. wavelength and stellar distance for G2 stars on the KIN. Also given is the equivalent OPD stability.

The specific requirement which the Keck Nuller has been designed to meet is the capability to detect an exo-zodiacal dust disk as faint as 10 (baseline requirement) to 30 (minimum requirement) times the level of our own solar system's zodiacal dust disk, around a G2 star at a nominal distance of 10 pc. For reference, a zodiacal dust disk 10 times as bright as that of our own solar system is roughly 10^{-3} as bright as a G2 star in the mid-infrared, and so suppression of the stellar signal to roughly the 10^{-3} level is needed. In the absence of errors, the stellar signal which will leak through an achromatic null fringe will be dominated by the leakage due to the finite size of the star, and this leakage, in the case of the 85 m Keck-Keck baseline, will be near 10^{-3} at a wavelength of 10 μm for G2 stars at a distance of 10 pc or greater.

(Figure 1). The targeted instantaneous nulling passband is 10 to 12 μm , but the various individual subsystems have been designed to operate throughout the N-band atmospheric window.

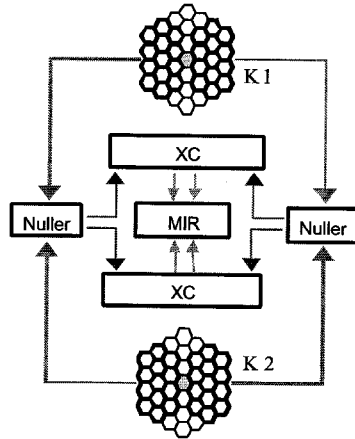


Figure 2. The KIN experiment architecture: dual-baseline nulling.

2. EXPERIMENT ARCHITECTURE

For a ground-based experiment aiming to detect faint emission in close proximity to a vastly brighter point source such as a star, two extraneous signals must be removed: the stellar flux itself, and thermal background emission from sources such as the terrestrial atmosphere and the ambient temperature optics. In the mid-infrared the latter emission is significantly brighter than the star. Since both of these sources need to be suppressed, two types of “subtraction” are planned. First, a nulling beam combiner (NBC) will be employed to reduce the stellar signal to the 10^{-3} level. However, because the nulling beam combiner will maintain a fixed phase, the residual off-axis flux will need to be modulated in some fashion in order to distinguish the desired signal from the thermal background. This will be accomplished by generating a dual-baseline nulloer using four distinct subapertures on the two Keck telescopes (Figure 2), and then cross-combining the nulled outputs with a standard interferometric beamcombiner³.

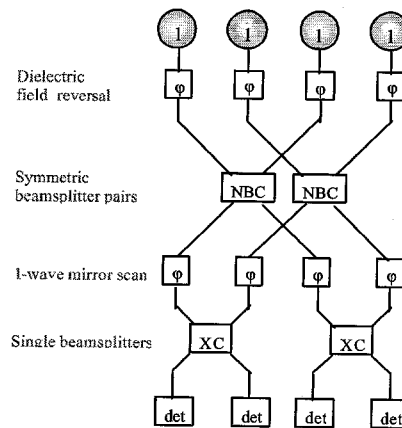


Figure 3. Conceptual layout of KIN dual-nuller, dual cross-combiner architecture. There are four input and output beams.

In other words, after the stellar signal is nulled on the pair of long baselines, the residual coherent off-axis signal from the astronomical target is modulated on the short baselines by means of a one-wavelength OPD scan in a pair of standard astronomical Michelson-interferometer beamcombiners (Figure 3). Thus the coherent exozodiacal signal is converted to an a.c. signal, while the incoherent thermal background signal remains at d.c., and so is not detected (it

does however contribute to the noise). This dual-nuller, dual cross-combiner architecture resembles some approaches being considered for TPF¹.

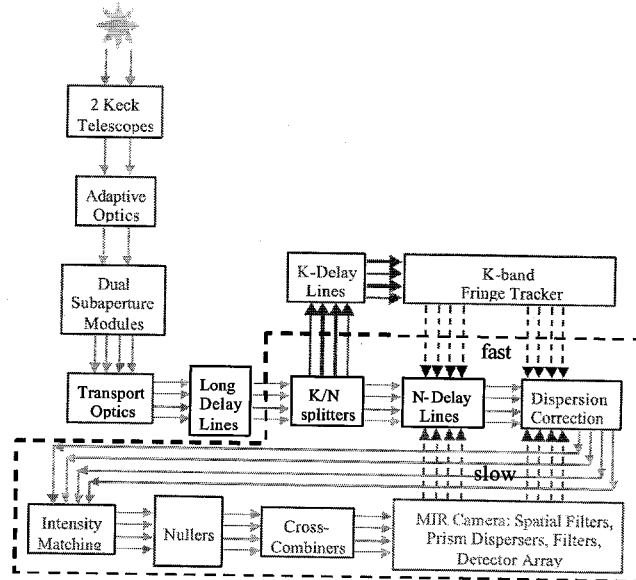


Figure 4. System layout. Components in the nulling subsystem are enclosed in the dashed line. Electrical signals are shown dashed.

The Keck Interferometer Nuller will make use of the interferometric infrastructure already deployed at the Keck Observatory⁴ as shown in Figure 4. The components in the dashed box are those related specifically to the nulling mode.

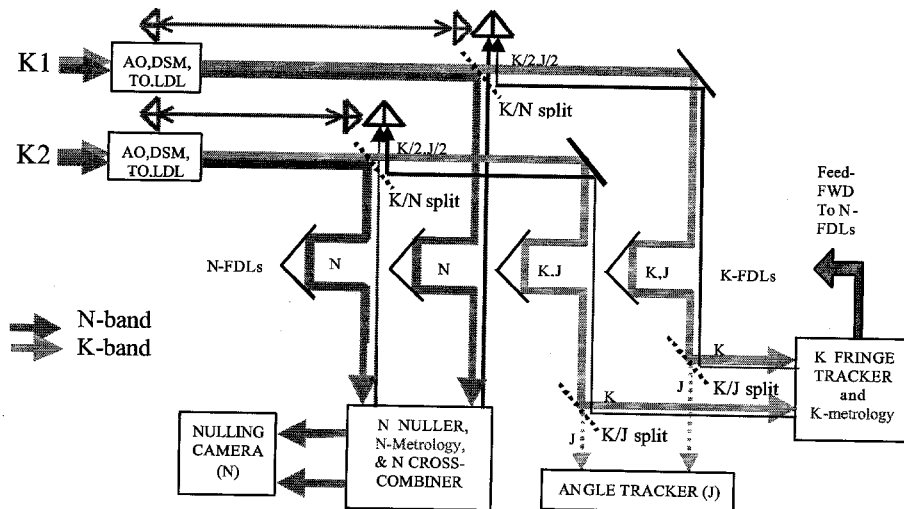


Figure 5. The KIN fringe-tracker and metrology layout

After traversing the adaptive optics systems, the light from the Keck primaries is split into a pair of symmetrical subapertures at the dual-subaperture modules. After propagation to the basement laboratory through a series of transport optics and long delay lines, the light is split between the K- and N-bands (2 μm and 10 μm , respectively). The K-band light is sent to a set of active delay lines, which is used to perform fringe tracking. The N-band light is sent to its own set of delay lines which are stabilized at the correct position by the information provided (fed-forward) by the K-band fringe tracker and the metrology signals. The latter, among other things, measure the non-common paths (Figure 5).

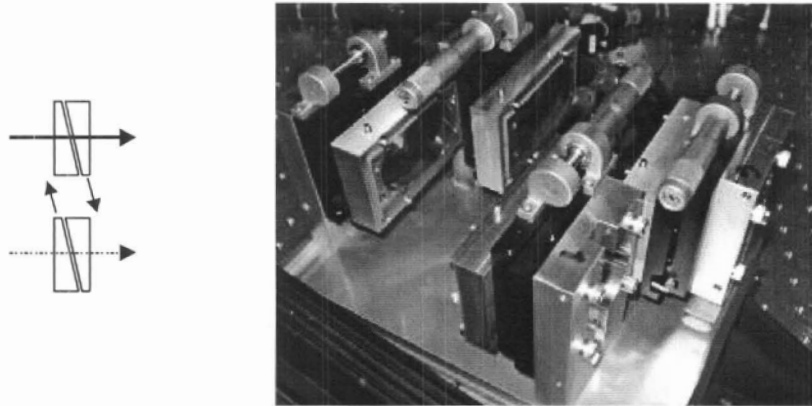


Figure 6. Unbalanced-dielectric (ZnSe) atmospheric dispersion compensators.

After the delay lines, the beams are compressed, and then pass through atmospheric dispersion compensators⁵ (which also add the necessary π -radian phase shift between the beams to be nulled), as shown in Figure 6. The beams then pass through intensity control devices (obscuring vanes), and proceed to the nulling beam combiners.

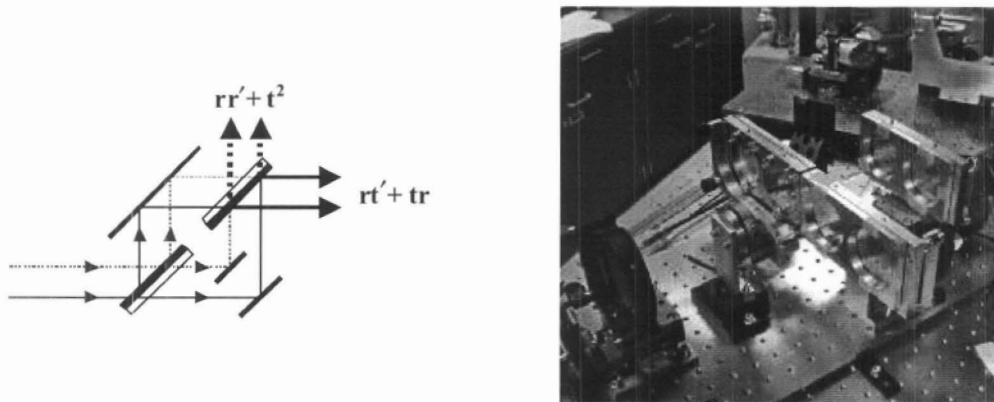


Figure 7. Modified Mach-Zehnder beam combiner

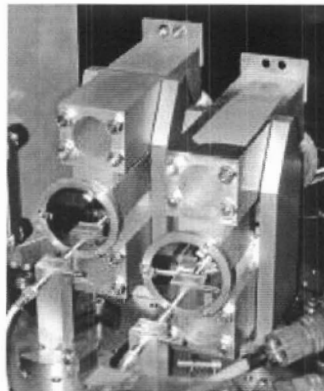


Figure 8. Cross-combiner rapid-scan mirrors

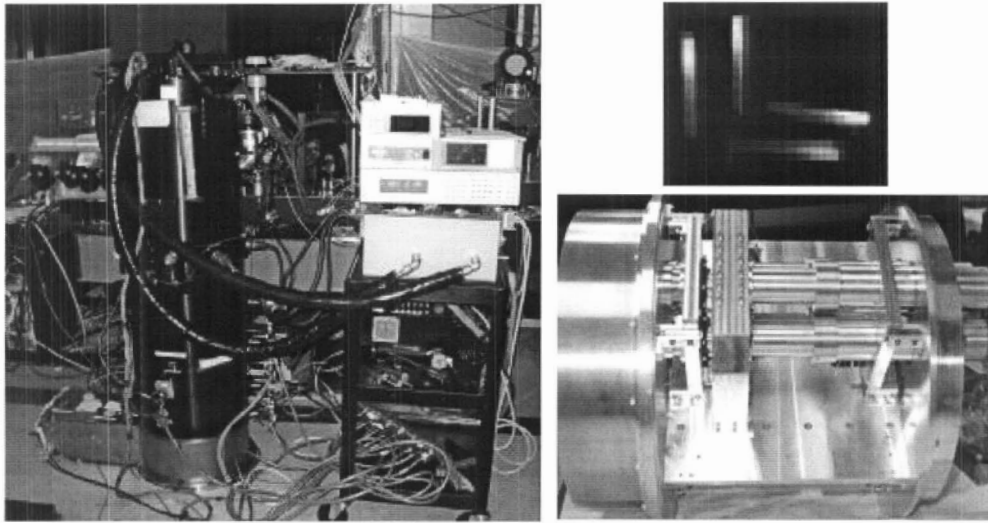


Figure 9. The KALI camera, its internal optics bench, and one output frame, showing the four dispersed channels.

The nulling beam combiners are symmetric modified Mach-Zehnder beamcombiners⁶ (Figure 7), which operate on the constructive fringe in the absence of the dispersion compensators. The nulled light is then passed to the cross-combiners, which consist of single beamsplitters, the associated compensator plates, and a pair of rapid-scan mirrors (Figure 8), which are capable of rapidly (100 Hz) scanning through an optical path difference (OPD) of a (mid-infrared) wavelength.

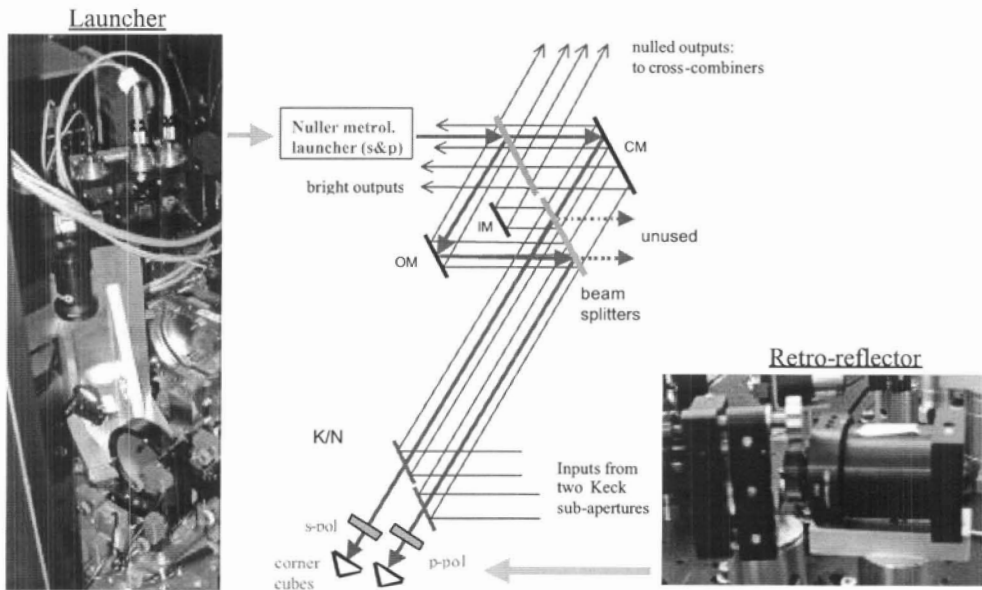


Figure 10. The KIN metrology system

After the cross-combiners, the light in the four destructive beams is sent to the mid-infrared camera KALI⁷ (Keck Aperture nUlling Interferometer camera), which provides spectral and spatial filtering, as well as a prism-based dispersion capability (Figure 9). The camera transmission was measured to be $\approx 50\%$ in the two best input beams.

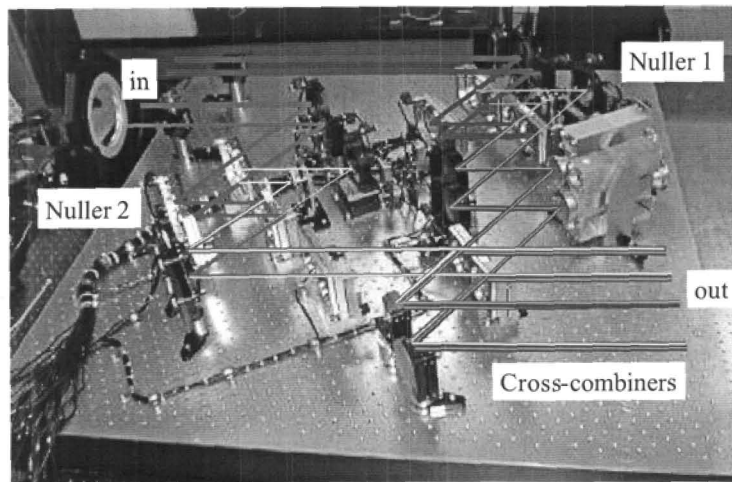


Figure 11. The nulling breadboard at an early assembly stage, showing only the nulling beam-combiners and the cross-combiners.

Metrology beams are launched from behind the final beamsplitters in the nulling beamcombiners (Figure 10), i.e., into one of the unused bright nuller outputs in each of the two nullers. The final beamsplitter splits the metrology beam and sends the two beams up the optical beamtrain. These beams are retro-reflected behind the K/N splitters, where linear polarizers select orthogonal polarizations in the two arms. By detecting the return metrology signals at both bright outputs in each nuller, all of the necessary paths can be monitored and stabilized. The metrology beams from the K-band fringe trackers also terminate at the retro-reflectors behind the K/N splitters, allowing for the stabilization of the non-common paths after these splitters. Another set of metrology beams monitors the common beam trains from the K/N splitters up to the dual-subaperture modules (Figure 5).

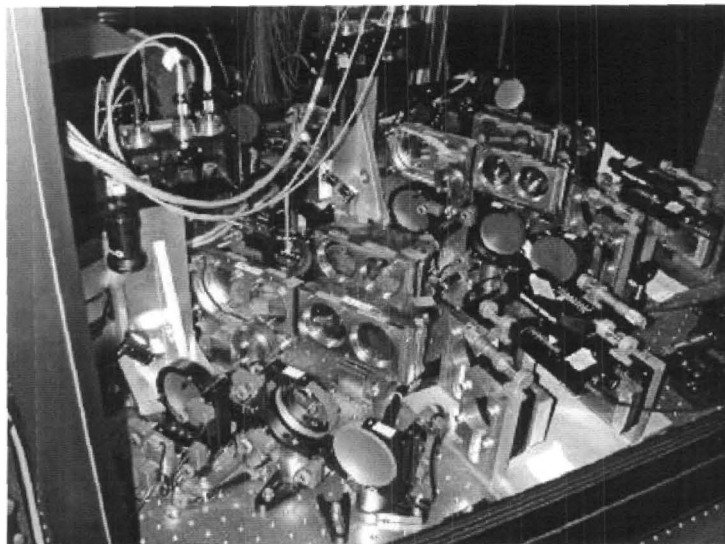


Figure 12. The fully assembled nulling breadboard.

Metrology is not presently provided for the cross-combiner stage because the OPD accuracy requirement for this stage is very relaxed compared to the nulling stage. However, the upgrade plan includes metrology for the cross-combiner stage if it is found to be necessary.

All of the nulling components are mounted on an enclosed four-foot square optical breadboard. Figure 11 shows the nullers and cross-combiners on the nulling breadboard in an early assembly phase, while Figure 12 shows the fully assembled system, including the dispersion compensators and metrology launchers. The transmission through the nulling breadboard optics was measured to be $\approx 80\%$. Finally, Figure 13 shows the full nulling subsystem, which includes the nulling breadboard, the source-plate, and the KALI camera, which sits on a mount on the floor next to the nuller table.

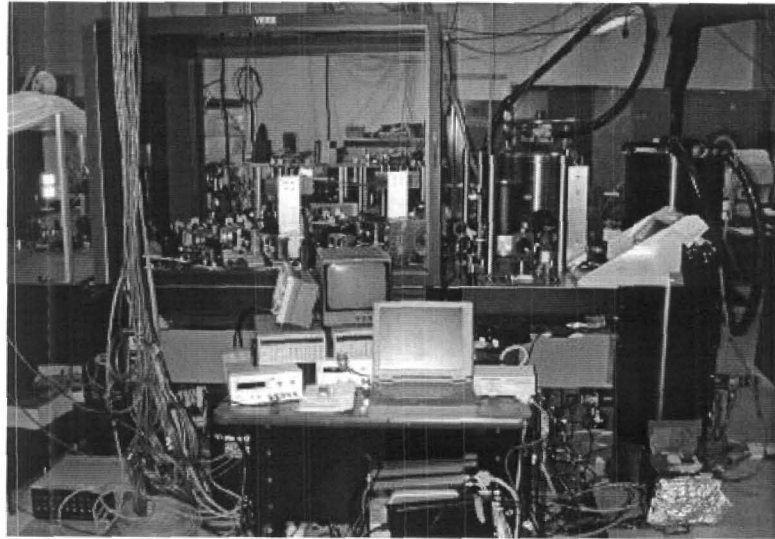


Figure 13. The nulling subsystem, showing the nulling breadboard (left) in its enclosure, the source plate (center), and the KALI camera (right; on the floor). The periscopes which drop the beams from the optical table to the bottom of the dewar can also be seen.

For laboratory testing, the thermal light source on the source plate (Figure 13) is injected into one of the four nuller outputs in the reverse direction⁶. Four beams propagating in the reverse direction are generated by the cross-combiner and nuller beamsplitters, and after retro-reflection at flat mirrors (located anywhere after the dispersion compensators, but for system tests these flats are located after the K/N splitters), four equivalent beams propagate toward the nulling breadboard in the forward direction, analogous to the incoming starlight.

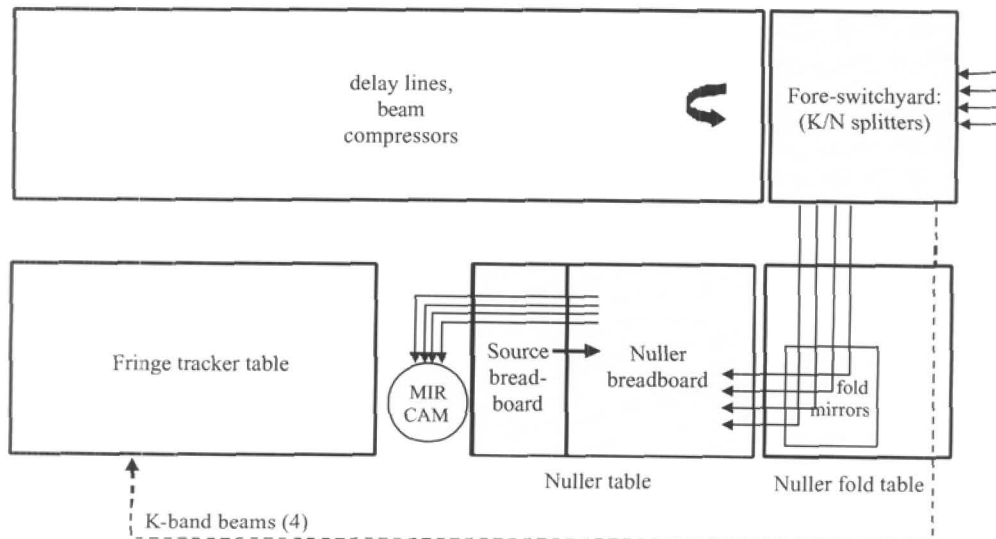


Figure 14. The summit basement layout. The nulling-specific subsystems are highlighted

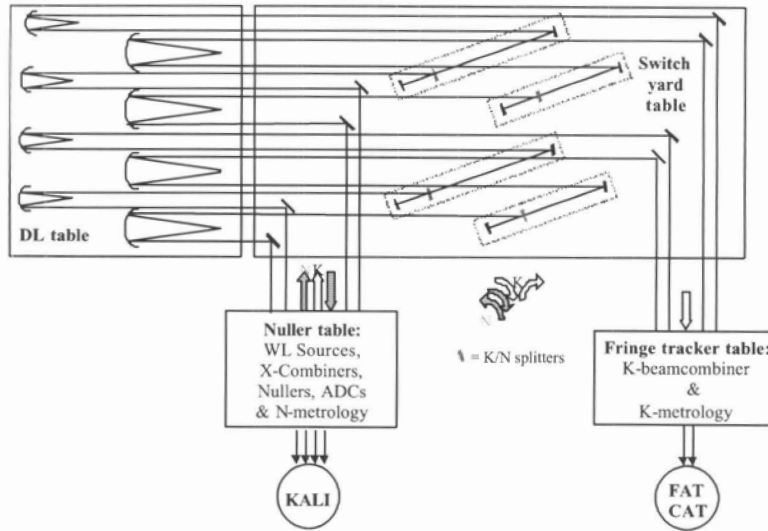


Figure 15. JPL I&T lab layout, showing the four optical tables involved, and the nulling and fringe-tracker cameras.

3. PERFORMANCE SUMMARY

The critical system-level performance demonstrations which were deemed necessary and sufficient to warrant shipment of the nulling hardware to the Keck Observatory were, in brief, demonstrations of suitable levels of null depth (1000:1), and null stability (several minutes at the desired rejection level), path-length stabilization by feed-forward from the K-band fringe tracker (FATCAT), and for the new KALI camera, the various normal camera functionality and performance standards such as encircled energy and sensitivity.

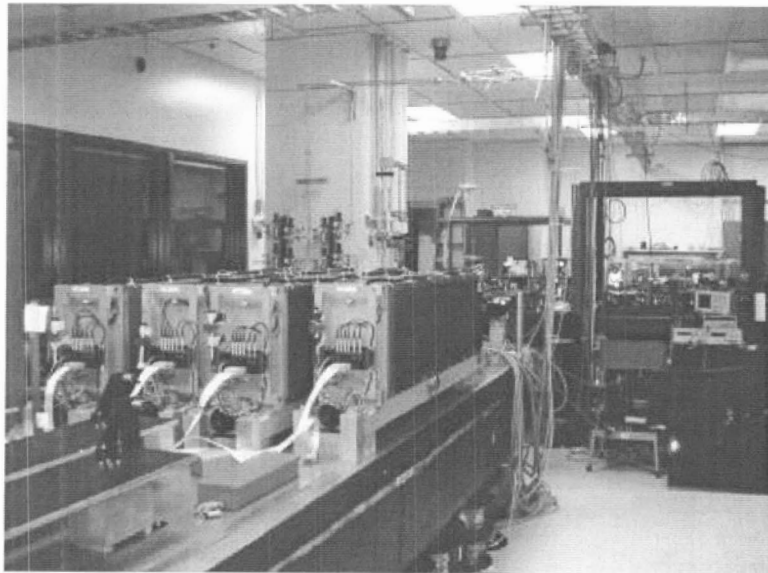


Figure 16. The I&T lab at JPL. The delay line table is front left, the switchyard table is in the center rear, the nulling breadboard (with enclosure) is on the right, and the fringe tracker table behind it (not visible). The full nulling table and the KALI camera, both to the right of this photo, are shown in Figure 13.

To carry out the needed interferometry-related demonstrations, the Keck Interferometer integration and test (I&T) laboratory at JPL was configured so as to reproduce the planned Keck Observatory basement layout and functionality (Figures 14, 15 & 16), including the K/N wavelength split, the relevant active delay lines, the metrology and alignment systems, the use of the KALI camera, and the use of summit-compatible real-time control software. In addition, an air path of order 20 m was of necessity included, as was the transit of the optical beams across a number of different optical tables, as will be the case on the summit. The summit block diagram layout is shown in Figure 14, the conceptual I&T lab layout is shown in Figure 15, and a photograph of the full I&T setup at JPL is shown in Figure 16.

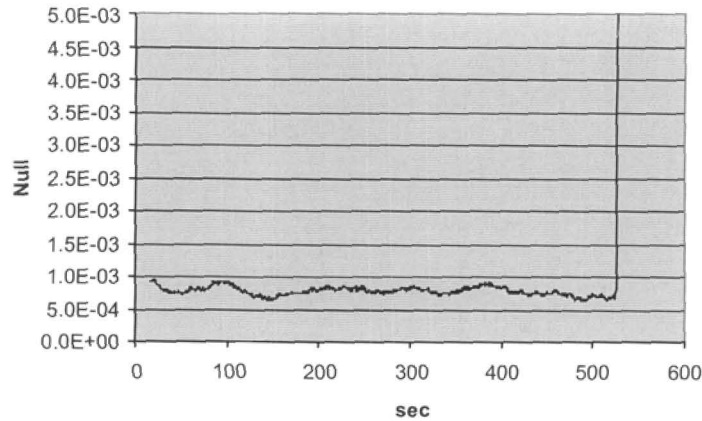


Figure 17. Metrology-stabilized system null depths obtained recently (June 2004) in the Keck Interferometer Lab at JPL, for a $2\ \mu\text{m}$ wide dispersed passband ($\approx 10 - 12\ \mu\text{m}$). After about nine minutes, the system was tuned to the constructive fringe.

The individual Keck nullers had already demonstrated null depths at the 10^{-4} level early last year^{3,8} (using a single-pixel detector and no metrology), and after an extended integration and test period, during which all of the other necessary subsystems were brought on line, system null depths of better than 10^{-3} were recently obtained, and stabilized for periods of many minutes (Figure 17). Feed-forward experiments from K-band to N-band at the requisite level were also successfully carried out.

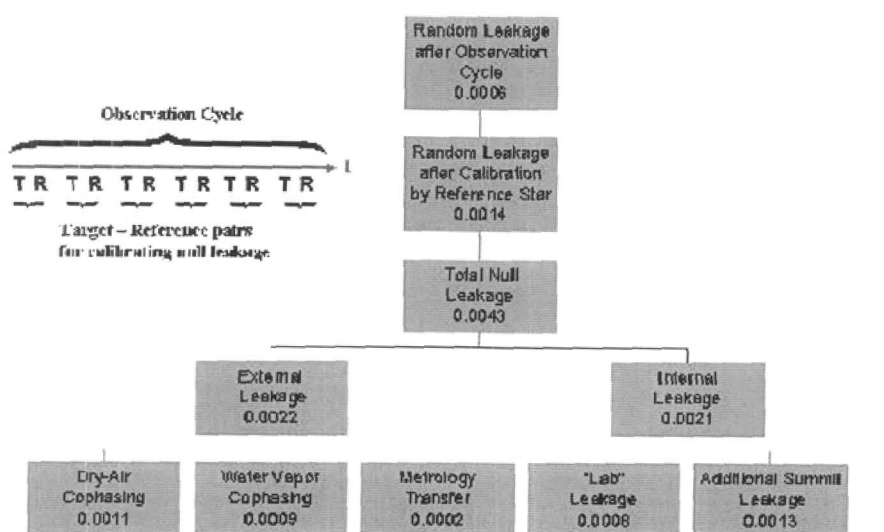


Figure 18. Predicted summit nuller error budget at initial performance levels.

Finally, with the experience gained in the I&T phase, it was possible to generate predictions for the initial summit performance. The results, as shown in the error budget in Figure 18, indicate that it should be possible to meet the on-sky nulling requirements with the hardware performance demonstrated in the I&T lab, assuming that our understanding of atmospheric water vapor fluctuations is accurate. This led to the decision to deploy the hardware to the Observatory.

ACKNOWLEDGEMENTS

This work was carried out at the Jet Propulsion Laboratory, California Institute of Technology, under contract with the National Aeronautics and Space Administration.

REFERENCES

1. C.A. Beichman, N.J. Woolf & C. Lindensmith 1999, JPL Publ. 99-3
2. Darwin – The Infrared Space Interferometer, 2000, ESA-SCI(2000)12
3. E. Serabyn, 2003, in *Toward other Earths*, ESA SP-539, p. 91
4. M.M. Colavita & P.L. Wizinowich 2002, in *Interferometry for Optical Astronomy II*, Proc. SPIE 4838, p. 79
5. C. Koresko et al. 2002, in *Interferometry for Optical Astronomy II*, Proc. SPIE 4838, p. 625
6. E. Serabyn 2002, in *Interferometry for Optical Astronomy II*, Proc. SPIE 4838, p. 594
7. M. Creech-Eakman et al. 2002, in *Instrument Design and Performance for Optical/Infrared Ground-Based Telescopes*, Proc. SPIE 4841, p. 330
8. B. Mennesson et al. 2003, in *Toward other Earths*, ESA SP-539, p. 525